CHAPTER 4

Synthesis and Applications of Water-Soluble Fluorescent Silver Nanoclusters

HANGXUN XU*[a] AND KENNETH S. SUSLICK*[b]

[a] CAS Key Laboratory of Soft Matter Chemistry, Department of Polymer Science and Engineering, University of Science and Technology of China, Hefei, Anhui, 230026, P. R. China; [b] Department of Chemistry, University of Illinois at Urbana-Champaign, Urbana, IL 61801 USA
*Email: hxu@ustc.edu.cn; ksuslick@illinois.edu

4.1 Introduction

AQ:1 AQ:2 Ag nanoclusters consisting of several to a hundred atoms with diameters less than 2 nm show molecule-like properties, including discrete electronic transitions and strong fluorescence.[1–4] They have received considerable research interest due to their unique optical, electrical and chemical properties and potential applications in chemical- and bio- sensing.[5–8] Ag nanoclusters exhibit excellent photostability, large Stokes shifts and high quantum yields, and therefore, they have become an important class of fluorophores for applications in imaging.[6,7] Since most applications involve aqueous conditions,[9] the synthesis of aqueous-stable and water-soluble Ag nanoclusters is critical. The synthesis of water-soluble Ag nanoclusters, however, is challenging because few-atom silver nanoclusters are highly reactive and will quickly aggregate to form large nanocrystals thus reducing their surface energy. Recently, many different synthetic approaches including radiolytic, chemical, sonochemical,

RSC Smart Materials No. 7
Functional Nanometer-Sized Clusters of Transition Metals: Synthesis, Properties and Applications
Edited by Wei Chen and Shaowei Chen

Published by the Royal Society of Chemistry, www.rsc.org

photochemical, and microwave methods have been developed to prepare water-soluble fluorescent Ag nanoclusters.[9] This chapter will highlight recent advances in the synthesis of water-soluble fluorescent Ag nanoclusters and briefly introduce their applications in chemical- and bio- sensing.

Historically, well before the development of modern analytical techniques, photographers were the first to generate and utilize Ag nanoclusters.[10,11] Photographers used papers impregnated with silver halides to make images even in the early nineteenth century. When a photographic emulsion containing silver halides was exposed to light, silver halides were decomposed to form Ag ions, bromine, and free electrons followed by formation of Ag crystals. Associated with this process, species like Ag_2^+, Ag_2^0, Ag_3^0, Ag_3^+, Ag_4^0, and Ag_4^+ were also generated.[11] This was believed to be the first chemical process to make reactive Ag nanoclusters, although photographers did not understand that Ag nanoclusters were formed nor did they realize that Ag nanoclusters consisting of few atoms were fluorescent. In the 1970s, discrete absorption and fluorescence from Ag nanoclusters were spectroscopically detected in cryogenic noble gas matrix.[12] During the condensation of Ag with Ar gas, excited Ag_2^* and Ag_3^* were formed and chemiluminescence was observed.[13] Ag nanoclusters formed under these extreme conditions, however, are not amendable to real world applications.

4.2 Synthesis of Water-Soluble Fluorescent Ag Nanoclusters

4.2.1 Radiolytic Reduction Synthesis of Ag Nanoclusters

Radiolytic reduction of Ag ions in aqueous solutions with common polyelectrolytes as stabilizers usually leads to the formation of large Ag nanoparticles with typical surface plasmon resonance bands around 380–400 nm. During short γ-ray irradiation, Henglein and co-workers observed the formation of Ag nanoclusters consisting of a few Ag atoms in the presence of polyphosphate or polyacrylate.[14–17] Ag nanoclusters obtained in this way exhibit absorption bands characteristic of Ag nanoclusters with a few Ag atoms at 275 nm, 300 nm, 330 nm, and 345 nm.[14] Unfortunately, Ag nanoclusters prepared *via* this approach were short lived and formed large Ag nanoparticles after several hours. Pulse radiolysis experiments indicated that Ag nanoclusters also form in the solution without stabilizers,[18] but the lifetimes of bare Ag nanoclusters were too short to be detected during the synthesis of Ag nanoparticles using the γ-ray irradiation method, and therefore the existence of Ag nanoclusters had been overlooked.

The formation of Ag nanoclusters in aqueous solutions under γ-ray irradiation is thought to proceed *via* the following process:

$$Ag^+ + e_{aq}^- \text{ or } R^\bullet \rightarrow Ag^0 \quad (1)$$

$$nAg^0 \rightarrow Ag_n \text{ (where } Ag_n \leq 2 \text{ nm for nanoclusters)} \quad (2)$$

Highly reactive species like radicals or solvated electrons can reduce Ag^+ to form Ag atoms in the solution. Meanwhile polyelectrolytes in the solution prevented the aggregation of Ag nanoclusters to form large Ag nanoparticles. Even so, these Ag nanoclusters were not stable and were very sensitive to UV light, being easily converted to large metallic Ag particles under UV irradiation.[15] In addition, Ag nanoclusters formed in this way were highly reactive due to the fact that the sizes of Ag nanoclusters were very small and essentially all Ag atoms were ''surface atoms''.[16] If a nucleophilic reagent such as NH_3, SH^- or CN^- is added to the Ag nanocluster solution, a strong absorption peak corresponding to Ag nanoparticles will quickly appear and all the characteristic absorption peaks of Ag nanoclusters disappear due to the conversion of Ag nanoclusters to Ag nanoparticles.[19]

Radiolytic reduction was able to fabricate water-soluble Ag nanoclusters conveniently, but Henglein and co-workers did not report the observation of fluorescence from Ag nanoclusters in aqueous solutions. A detailed study of the fluorescence properties of water-soluble Ag nanoclusters produced by radiolytic irradiation of Ag^+ was only recently published in 2005 by Treguer *et al.*[20]

4.2.2 Photochemical Reduction Synthesis of Ag Nanoclusters

The fluorescence of Ag nanoclusters in the solid state was first observed by photochemical reduction of AgO films by Dickson and co-workers in 2001.[21] In this case, fluorescent Ag nanoclusters were formed by light-induced decomposition of AgO. They also first reported the preparation of water-soluble fluorescent Ag nanoclusters *via* a photochemical reduction method using dendrimers as stabilizers.[22] Ag nanoclusters prepared in this way exhibited much narrower and more stable emission spectra than those individual Ag nanoclusters observed in AgO films.

For the formation of Ag nanoclusters *via* UV irradiation it is crucial that there be polymeric capping agents in solution. A variety of polyelectrolytes with simple structures can be used to prepare water-soluble fluorescent Ag nanoclusters *via* a photochemical approach; for example, highly fluorescent Ag nanoclusters were synthesized in aqueous solutions containing polyelectrolytes such as poly(methacrylic acid) (PMAA) and poly(acrylic acid) (PAA).[23] Ag nanoclusters obtained in this way exhibited excitation-dependent emission, relatively high quantum yield, and good photostability. Interestingly, these Ag nanoclusters also showed solvato-fluorochromic properties and were electrochemiluminescent (Figure 4.1).[24] The optical absorption and fluorescence emission properties of Ag nanoclusters prepared in this way can be tuned by choice of solvent. When the solvent was changed from water to methanol, a $\sim$70 nm red shift of the absorption peak was observed. In addition, these Ag nanoclusters also showed cathodic hot electron-induced electrochemiluminescence. This phenomenon was believed to proceed *via* a redox excitation pathway, where the Ag nanoclusters were oxidized by the cathodically produced oxidizing radicals in the solution. In a

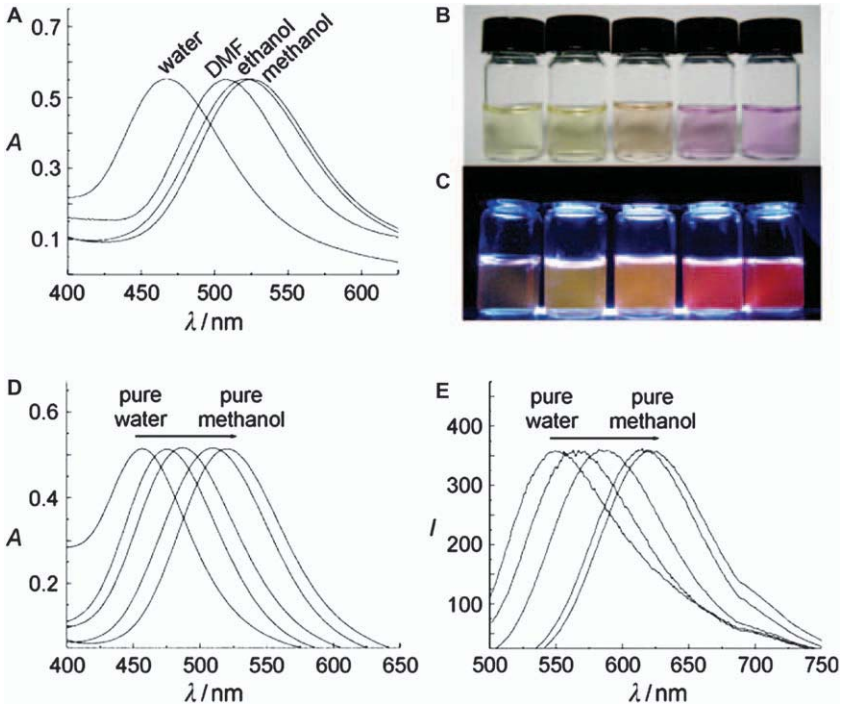

Figure 4.1 (A) UV-Vis absorption spectra of Ag nanoclusters in different solvents. Ag nanoclusters in water–methanol mixtures ranging from pure water (left) to pure methanol (right) under (B) visible light and (C) UV light illumination. (D) Absorption and (E) emission spectra of Ag nanoclusters shown in (B).
Reproduced with permission from ref. 24. Copyright 2009 John Wiley & Sons.

similar approach, poly(methacrylic acid) functionalized with pentaerythritol tetrakis-3-mercaptopropionate (PTMP–PMAA) was successfully used to prepare water-soluble Ag nanoclusters *via* a photochemical reduction method.[25] This polymer can also be used to make other water-soluble fluorescent metal nanoclusters like Cu nanoclusters and Au nanoclusters.

Polymer microgels (poly(*N*-isopropylacrylamide-acrylic acid-2-hydroxyethyl acrylate)) and multiarm star polyglycerol-*b*-polyacrylic acid (PG-*b*-PAA) copolymers were also used as templates to synthesize water-soluble fluorescent Ag nanoclusters using photochemical reduction.[26,27] The optical properties and photoluminescence of Ag nanoclusters prepared in the interior of macromolecular templates can be finely controlled using appropriate UV-irradiation time. Because both templates contain pH or temperature sensitive polymers, the fluorescent properties of Ag nanoclusters can be additionally tuned using external stimuli (*i.e.*, pH and temperature). Photochemical reduction is a clean synthetic approach and avoids the addition of external reducing agents.

4.2.3 Sonochemical Preparation of Ag Nanoclusters

Similar to the effects of γ-ray and deep-UV irradiation, highly reactive species like $OH^{\bullet}$, $H^{\bullet}$, $HO_2^{\bullet}$, and perhaps solvated electrons, e_{aq}^- are formed during ultrasonic irradiation of aqueous solutions.[28–30] High intensity ultrasound has found many important applications in the synthesis of nanostructured materials.[31,32] Extreme conditions inside collapsing bubbles with temperatures up to 20 000 K and pressures as high as 4000 bar have been spectroscopically determined during single-bubble cavitation.[33] The implosive collapse of cavitating bubbles can generate a number of reactive species that are chemically reductive and can be used to reduce Ag^+ in the solution.

Sonication of aqueous $AgNO_3$ solutions with dissolved PMAA easily forms fluorescent Ag nanoclusters.[34] The optical and fluorescence properties of Ag nanoclusters can be controlled by varying the duration of sonication (Figure 4.2). Prolonged sonication resulted in the formation of large Ag nanoparticles with a surface plasmon resonance band at 390 nm and decrease of the fluorescence intensity. TEM images indicate that all the sonochemically prepared Ag nanoclusters were smaller than 2 nm in diameter (Figure 4.2) and that the sizes of Ag nanoclusters increased as the sonication time increased. Sonochemically synthesized Ag nanoclusters exhibit excitation-dependent fluorescence. Varying the stoichiometry of the carboxylate groups relative to Ag^+ and the polymer molecular weight can also change the absorption and fluorescence of Ag nanoclusters prepared in this way. The quantum yield is measured to be ~11%. Thus, sonochemistry provides a uniquely simple approach to make water-soluble Ag nanoclusters with various optical and fluorescence properties.

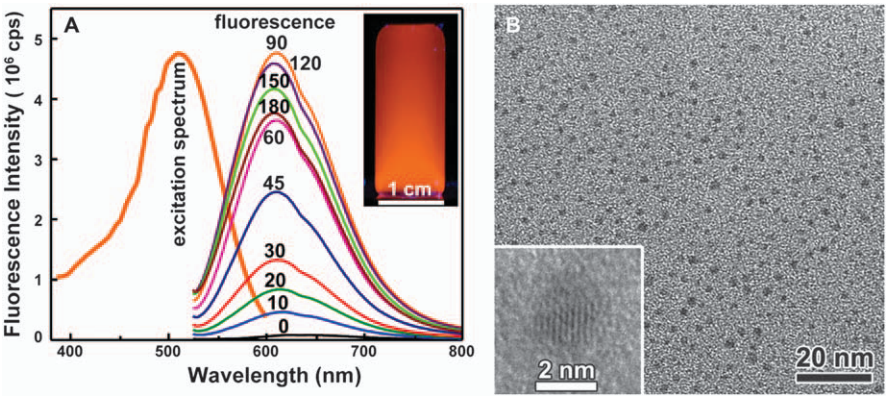

Figure 4.2 (A) Fluorescence emission spectra of sonochemically prepared Ag nanoclusters with sonication time varying from 0 to 180 min (inset: vial containing sonochemically prepared Ag nanoclusters illuminated by a 365 nm UV lamp). (B) TEM images of as-prepared Ag nanoclusters after 90 min sonication (inset shows a single magnified Ag nanocluster). Reproduced with permission from ref. 34. Copyright 2010 American Chemical Society.

4.2.4 Microwave-Assisted Synthesis of Ag Nanoclusters

Microwave irradiation is becoming an important tool in daily life and even in chemical reactions. The first use of microwaves as a heating method in chemical modifications can be traced back to the 1950s.[35] Microwave-assisted synthesis has gained wide acceptance since the report of using microwave irradiation in organic synthesis in 1986 and results primarily from rapid superheating of solvents.[36] The use of microwave heating for organic synthesis and chemical preparation of nanostructured materials has been extensively investigated in recent decades. Recently, microwave irradiation has also been applied to the synthesis of water-soluble fluorescent Ag nanoclusters.

Microwave irradiation of a PMAA solution with Ag^+ provided a rapid synthetic approach to prepare water-soluble fluorescent Ag nanoclusters (fluorescence appeared in 30 s).[37,38] The as-prepared Ag nanoclusters exhibited strong fluorescence emission at 575 nm with excitation at 510 nm (Figure 4.3A).[37] TEM imaging indicated that Ag nanoclusters prepared in this way were monodisperse and highly uniform with a diameter around 2 nm (Figure 4.3B).[37] The quantum yield was measured to be ~6%. The fluorescence of Ag nanoclusters prepared using the microwave irradiation method varied with different irradiation time. The fluorescence intensity gradually increased up to 70 s of irradiation and then gradually decreased until it completely disappeared after 140 s. In addition to the duration of microwave irradiation, the solution pH also affected the fluorescence properties of Ag nanoclusters. Maximum intensity was achieved when the initial pH was ~7. Water-soluble Ag nanoclusters prepared using microwave irradiation showed high selectivity for sensing Cr^{3+} ion in aqueous solutions.[37] Microwave-assisted synthesis offers a unique means for rapid and

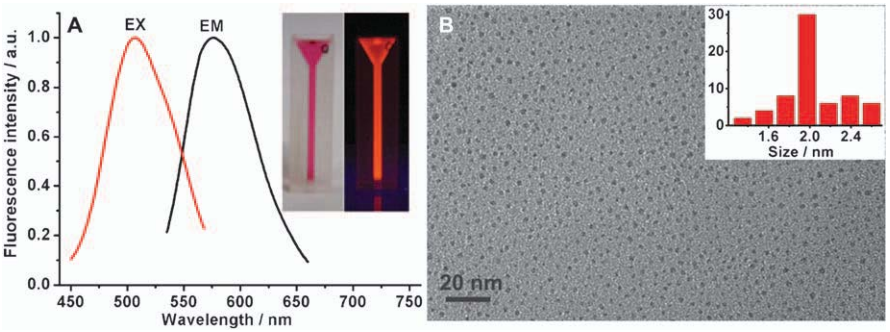

Figure 4.3 (A) Excitation and emission spectra of Ag nanoclusters synthesized *via* microwave irradiation (inset shows photographs of a solution of Ag nanoclusters under room light and 365 nm UV light illumination). (B) A typical TEM image of highly fluorescent Ag nanoclusters (inset shows the diameter histogram of Ag nanoclusters).
Reproduced with permission from ref. 37. Copyright 2011 Royal Society of Chemistry.

uniform heating of solutions; therefore, it can generate more homogeneous nucleation and shorter crystallization time for nanoclusters.

4.2.5 Chemical Reduction for Preparation of Ag Nanoclusters

Water-soluble Ag nanoclusters can be obtained through chemical reduction of Ag^+ using $NaBH_4$ in aqueous solutions or by bubbling an alkaline Ag^+ solution with H_2 and CO in the presence of polyphosphate.[16] Such chemical reduction methods, however, simultaneously produced large metallic Ag nanoparticles in the solution as confirmed by a strong absorption band at 380 nm corresponding to Ag nanoparticles. The reason for the formation of metallic Ag nanoparticles is probably the rapid aggregation of synthesized Ag nanoclusters due to the lack of appropriate stabilizers.

To avoid the formation of Ag nanoparticles in this process, the presence of stabilizers with high affinity for Ag^+ in the solution is necessary. DNA, peptides, proteins, and polythiol- or polyamine- appended molecules are commonly used stabilizers when chemical reduction is used to make water-soluble fluorescent Ag nanoclusters. DNA was the first used by Dickson *et al.* as a template to produce stable, water-soluble, nanoparticle-free, and fluorescent Ag nanoclusters with $NaBH_4$ as the reducing agent.[39–41] Ag^+ ions have strong interactions with oligonucleotide bases (N3 in the pyrimidines and N7 in the purines) but not with the negatively charged phosphates of the backbone. Upon adding $NaBH_4$ to the mixture of DNA and silver nitrate, small Ag nanoclusters were formed and no nanoparticles were observed. Mass spectral analysis indicated that this approach produced a maximum of 4 Ag atoms in the DNA template. ^1H NMR spectra revealed that peaks corresponding to cytosine H5 and H6 were significantly shifted upfield, indicating that Ag had a high affinity for cytosine bases on single-stranded DNA. AQ:4 Circular chroism (CD) results also proved that Ag nanoclusters had high affinity with nucleobases, especially with cytosine. As a result, oligonucleotide strands used in the preparation of Ag nanoclusters usually contained a high percentage of cytosines in their sequences. Single-stranded DNA consisting of 12 cytosine bases were found to generate high quantum yield, near-IR emitting Ag nanoclusters (Figure 4.4).[40] The quantum yield of Ag nanoclusters prepared in this way was 17%. Chemical reduction preparations of Ag nanoclusters using DNA as a template exhibit excellent photostability and show essentially no photoblinking on experimentally relevant time scales (0.1 to >1000 ms).

Due to the fact that there were a number of different Ag nanoclusters formed with various numbers of Ag atoms, multiple emitting (red and blue–green) species were detected when the cytosine-rich oligonucleotide was used as a template. When 3 different oligonucleotides (dT_{12}, $dT_4C_4T_4$ and $dC_4T_4C_4$, where T = thymine and C = cytosine) were employed to make fluorescent Ag nanoclusters, both absorption and fluorescence spectral results indicated that thymine-rich oligonucleotides directed the formation of Ag nanoclusters that showed only blue–green emission, whereas

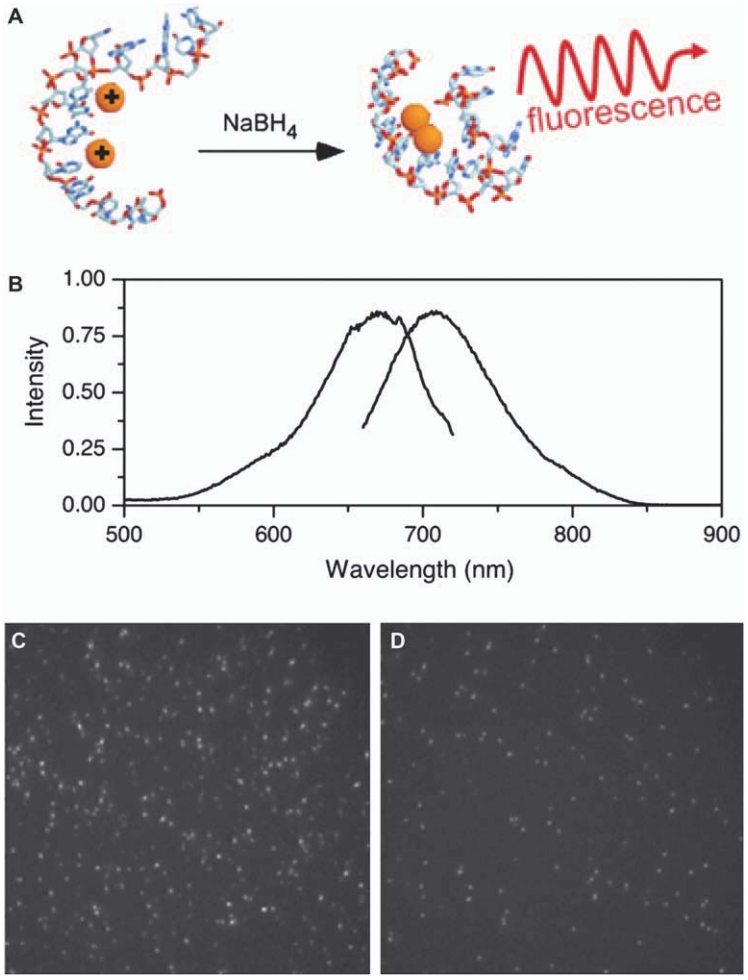

Figure 4.4 (A) Schematic illustration of the formation of Ag nanoclusters. After complexation of Ag^+ to single strand DNA containing 12 cytosines, the mixture was reduced with $NaBH_4$ and the fluorescent Ag nanoclusters formed. (B) Normalized excitation and emission spectra of the Ag nanoclusters. (C) Images of single Ag nanoclusters in a poly(vinyl alcohol) (PVA) film. (D) For comparison, the fluorescent image of single Cy5.29 molecules (a common fluorophore) in a PVA film. The image dimensions are 40 ìm×40 μm, and imaging conditions of (C) and (D) are identical.
Reproduced from ref. 40. Copyright 2007 American Association for the Advancement of Science.

cytosine-rich oligonucleotides led to the formation of both red- and blue–green emitting Ag nanoclusters.[42] This study indicated that base sequence influenced the fluorescence of Ag nanoclusters. Sequence-dependent fluorescence from Ag nanoclusters with different sequences and secondary

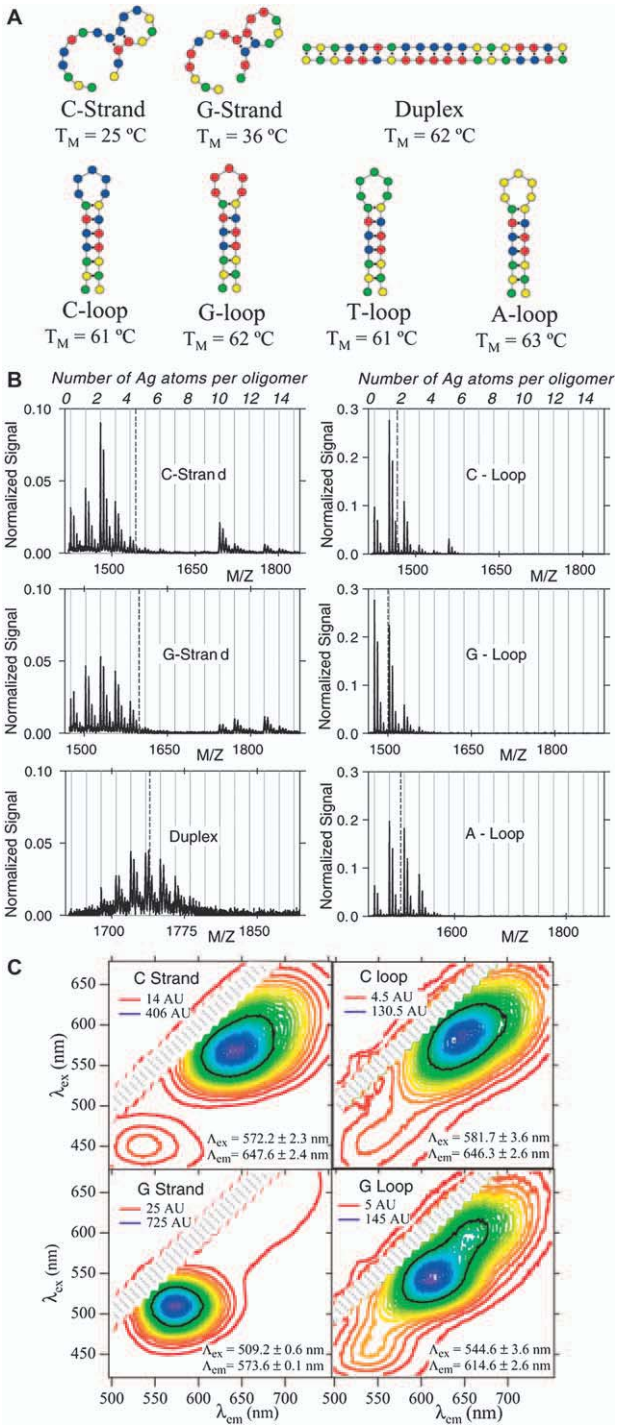
A
C-Strand
T_M = 25 ºC
G-Strand
T_M = 36 ºC
Duplex
T_M = 62 ºC
C-loop
T_M = 61 ºC
G-loop
T_M = 62 ºC
T-loop
T_M = 61 ºC
A-loop
T_M = 63 ºC
B
Number of Ag atoms per oligomer
Normalized Signal
C-Strand
C - Loop
G-Strand
G - Loop
Duplex
A - Loop
M/Z
C
C Strand
14 AU
406 AU
C loop
4.5 AU
130.5 AU
G Strand
25 AU
725 AU
G Loop
5 AU
145 AU
λ_{ex} (nm)
λ_{em} (nm)
Λ_{ex} = 572.2 ± 2.3 nm
Λ_{em}= 647.6 ± 2.4 nm
Λ_{ex} = 581.7 ± 3.6 nm
Λ_{em}= 646.3 ± 2.6 nm
Λ_{ex} = 509.2 ± 0.6 nm
Λ_{em}= 573.6 ± 0.1 nm
Λ_{ex} = 544.6 ± 3.6 nm
Λ_{em}= 614.6 ± 2.6 nm

structures of the bases that comprised the DNA strand was further investigated by Gwinn *et al.* using six 19-base DNA oligomers (Figure 4.5).[43] The fluorescence intensities and maximum emission peaks can be finely controlled by the DNA sequences and their secondary structures. Only one emission peak was observed when Ag nanoclusters were synthesized using the smallest hairpin. Other sequences, however, generated multiple emission peaks. Four different types of fluorescent Ag nanoclusters possibly containing different numbers of Ag atoms can be distinguished based on the fluorescence wavelengths and chemical stability. Gwinn *et al.* found that red and green emissions derived from Ag nanoclusters with 13 and 11 atoms respectively when DNA hairpin with 9 cytosines in the loop was used.[43] Microarrays with different DNA sequences were applied to identify the emission properties of Ag nanoclusters generated *in situ*. It was found that sequences indeed can induce the generation of Ag nanoclusters with different emission peaks from visible to near-IR. Therefore, the precise control of the fluorescent properties of Ag nanoclusters may become possible through choice of specifically designed DNA sequences and structures.

Ag nanoclusters were also used to make a fluorescence logic gate with the G-quadruplex in combination with a hairpin and i-motif.[44] The DNA used can fold into a hairpin with a C-loop and it also had several guanines in the stem. Therefore, this DNA can form a G-quadruplex upon the addition of K^+ in the solution. In addition, the DNA strand can generate an i-motif due to the presence of cytosines when the solution pH is lowered. Ag nanoclusters prepared at the hairpin state showed fluorescence peaks at 570 nm and 640 nm. When K^+ was added, only the 570 nm peak was strong. Lowering the solution pH completely quenched the fluorescence, and addition of K^+ and acid led to an emission peak at 601 nm. This ion-tuned fluorescence logic gate based on Ag nanoclusters can be illustrated in Scheme 4.1.[44] The fluorescence properties of Ag nanoclusters were also used to prepare logic devices based on programmable DNA-regulated Ag nanocluster signal transducers.[45] Using the DNA-encoding strategy, aqueous Ag nanoclusters were used as signal transducers to convert DNA inputs into fluorescence outputs for the construction of various DNA-based logic gates (AND, OR, INHIBIT, XOR, NOR, NAND, *etc*.) (Scheme 4.1). Because Ag nanoclusters can interact with many other biomolecules such as peptides, proteins, and RNA and are responsive to external stimuli, this kind of logic device may lead to a new generation of signal transducers and could be used to fabricate a variety of biomolecular logic systems.

Figure 4.5 (A) Schematic representations of the 19-base DNA oligomers used by Gwinn *et al.* Blue = cytosine (C), green = thymine (T), red = guanine (G), and yellow = adenine (A). (B) Mass spectra of the DNA–Ag solutions, for DNA sequences as labeled. (C) Contour maps of fluorescence emission *vs.* excitation from the DNA–Ag solutions. The black contour lies at the half-maximum intensity.
Reproduced from ref. 43. Copyright 2008 John Wiley & Sons.

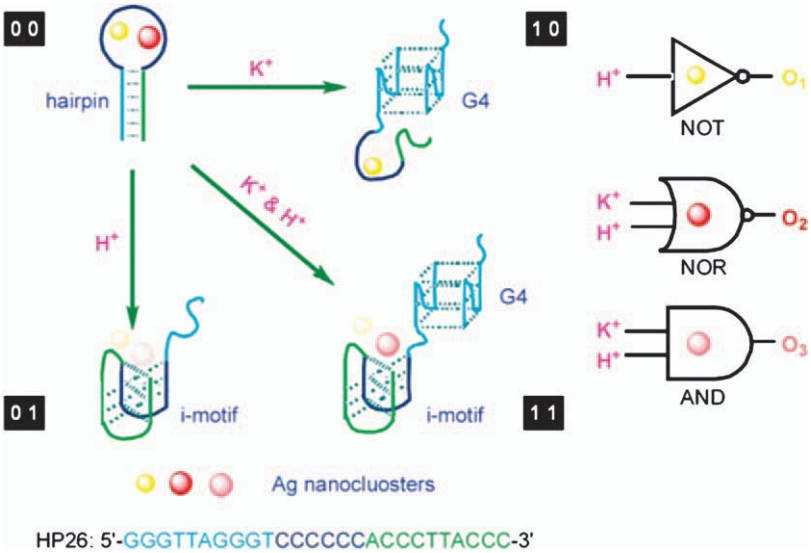

Scheme 4.1 (Left) Schematic chemical diagram of logic operations based on HP26-tuned fluorescent Ag nanoclusters. (Right) Corresponding symbols of logic gates. K^+ and H^+ serve as two independent inputs to trigger the allosterism of HP26 and modulate the fluorescence output. Ag nanoclusters are shown as spheres.
Reproduced with permission from ref. 44. Copyright 2011 American Chemical Society.

AQ:5 Lipoic acid and polyethylene glycol (PEG) modified lipoic acids are another class of versatile ligands for the synthesis of water-soluble fluorescent Ag nanoclusters.[46–48] Lipoic acid is not soluble in aqueous solutions. To make it soluble and stabilize aqueous Ag nanoclusters, $NaBH_4$ was required to reduce lipoic acid to form dihydrolipoic acid, which is soluble in water and can adsorb on the surface of Ag nanoclusters. High-resolution mass spectral study indicated that Ag nanoclusters prepared in this way primarily consisted of Ag_4 and Ag_5. PEG modified lipoid acids showed the capability to control the size of Ag nanoclusters *via* varying the stoichiometry of the Ag^+ to the ligands. Nanoparticles were formed for Ag to ligand ratios between 1000 and 5, while Ag nanoclusters were obtained for Ag to ligand ratios between 1 and 0.1 (Figure 4.6).[48] The unique advantage of using PEG modified ligands was the ability to control the surface functionalities of Ag nanoclusters *via* using different functionalized PEG ligands. For example, AQ:6 carboxylate and amine terminated PEGs can be. Surface functionality of Ag nanoclusters is very important because this allows further fine tuning of the reactivity of Ag nanoclusters with target molecules like proteins, peptides, and DNA. One might expand this procedure to potential applications of Ag nanoclusters in biological sciences.

Size focusing or core etching methods using PEG modified lipoic acids as stabilizing agents have also been developed.[48] Unlike other synthetic

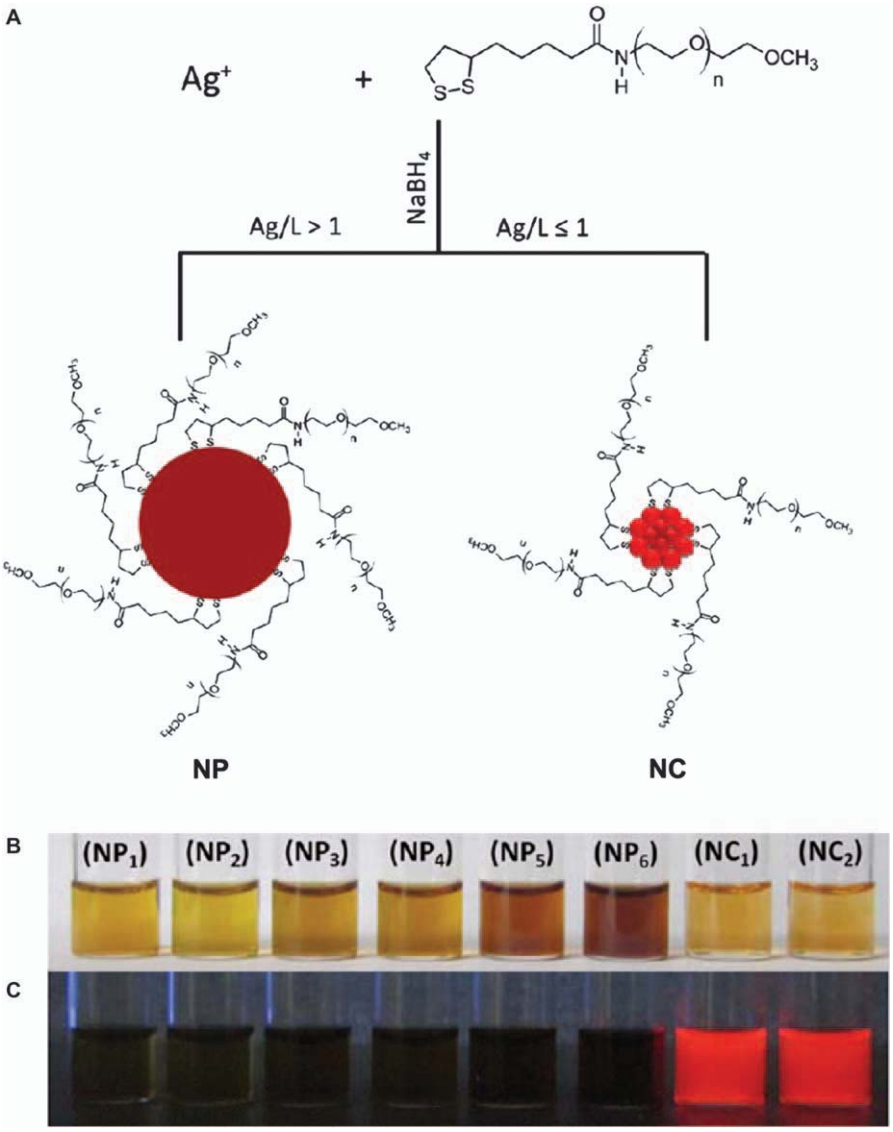

Figure 4.6 (A) Synthetic strategy of Ag nanoparticles and nanoclusters with different core sizes. The Ag to ligand ratios are varied to control the formation of either Ag nanoparticles or nanoclusters. (B) and (C) Photographs of aqueous solutions of Ag nanoparticles and nanoclusters synthesized at various Ag to ligand ratios under room light and UV irradiation, respectively.
Reproduced with permission from ref. 48. Copyright 2012 American Chemical Society.

approaches that all use Ag^+ as the nanocluster precursors, the size focusing method uses pre-formed Ag nanoparticles as precursors. Relatively large amount of ligands were required in this top-down route. TEM images clearly demonstrated that Ag nanoparticles with a rather broad size range ($\sim$2–7 nm) were reduced in size down to Ag nanoclusters with an average diameter of $\sim$1.3 nm. The exact mechanism for the conversion of Ag nanoparticles to Ag nanoclusters was not clear but this process is probably due to etching of Ag nanoparticles with excess free thiols in the solution leading to reduction in size and polydispersity.[48]

Other organic ligands have also been used to synthesize water-soluble fluorescent nanoclusters *via* chemical reduction. For example, a multistage ''cyclic reduction under oxidative conditions'' (with the dubious acronym, CROC) approach has been applied to prepare Ag nanoclusters with water-soluble chiral thiols (captopril ((2*S*)-1-[(2*S*)-2-methyl-3-sulfanylpropanoyl]pyrrolidine-2-carboxylic acid), glutathione (GSH = γ-Glu-Cys-Gly), and cysteine) as strong protecting and stabilizing ligands.[49] In this synthetic approach, $NaBH_4$ was used as the reducing agent and hydrogen peroxide was used as an oxidizing agent. Mass spectral analysis indicated that Ag nanoclusters prepared in this way primarily consisted of 22–28 Ag atoms. A protein stabilizer, bovine pancreatic α-chymotrypsin (CHT), was also developed for preparing fluorescent Ag nanoclusters of 1 nm average diameter.[50] In a kinetically controlled manner, Ag nanoclusters with less than 10 Ag atoms were obtained in microemulsions using $NaH_2PO_2 \cdot H_2O$ as a mild reducing agent.[51]

4.3 Applications of Water-Soluble Fluorescent Ag Nanoclusters

4.3.1 Applications of Ag Nanoclusters in Chemical Sensing

The fluorescence of water-soluble Ag nanoclusters is highly sensitive to local changes in their microenvironment, and can be employed to prepare highly sensitive fluorescent chemical and biological sensors in aqueous conditions. There are numerous recent reports on the applications of fluorescent Ag nanoclusters for sensing inorganic ions and biomolecules.

Cu^{2+} is an environmental pollutant and also a key trace element in biological systems. Photochemically produced Ag nanoclusters stabilized by PMAA were first used to detect Cu^{2+}.[52] The limit of detection (LOD, $s/n = 3$) was 8 nM, which is significantly lower than the EPA limit for Cu^{2+} in drinking water. The quenching of fluorescence was due to the complex formation between Cu^{2+} and carboxylic groups around fluorescent Ag nanoclusters. DNA-templated Ag nanoclusters were also developed for quantitative determination of Cu^{2+} in a label free format.[53] Such DNA–Ag nanoclusters showed a maximum fluorescence emission peak at 624 nm that quickly decreases upon the addition of Cu^{2+}. Further experiments indicated that the dominant factor causing the quenching of fluorescence was mainly the metal–metal interaction between Ag and Cu. The detection limit of this

method is 10 nM. Cu^{2+} can also be detected using DNA-templated Ag nanoclusters *via* a ''turn-on'' approach.[54] The introduction of Cu^{2+} resulted in the formation of DNA–Cu/Ag nanoclusters with enhanced fluorescence and much higher quantum yield. Although 3-mercaptopropionic acid (MPA) can quench the fluorescence of Ag nanoclusters, the MPA induced fluorescence quenching of DNA–Cu/Ag nanoclusters was suppressed by Cu^{2+} *via* reduction of thiols to form disulfide which was not able to interact with Ag nanoclusters to quench their fluorescence. This method allowed ''turn-on'' detection of Cu^{2+} at concentrations as low as 2.7 nM.

Water-soluble fluorescent Ag nanoclusters can also be used as Hg^{2+} sensors due to the strong fluorescence quenching capability of Hg^{2+}.[55,56] The LOD of lipoic acid capped Ag nanoclusters was measured to be 0.1 nM which is substantially lower than the maximum permissible concentration limit of Hg^{2+} in drinking water (10 nM), set by US EPA.[46] The fluorescence quenching of Ag nanoclusters may occur through Hg^{2+} mediated interparticle aggregation. A ''turn-on'' approach to Hg^{2+} detection has also been developed based on specifically designed DNA making use of the T–T mismatch coordinating capability of Hg^{2+}.[57] A single strand DNA with an inner C-loop was first hybridized to another single strand sequence of DNA with a few T mismatches around the loop. The Ag nanoclusters synthesized using this designed DNA only exhibited weak fluorescence. Upon addition of Hg^{2+}, however, a T–Hg^{2+}–T coordination was formed which increased the duplex stability and changed the environment around the C-loop. This structure change caused dramatic enhancement of fluorescence intensity thereby allowing highly sensitive detection of Hg^{2+} in aqueous solutions.[57]

Selective sensing of Cr^{3+} in aqueous solutions has been reported[37] with Ag nanoclusters prepared using a microwave-assisted method with PMAA as stabilizer. Cr^{3+} readily quenches fluorescent Ag nanoclusters at relatively low concentrations and the detection limit was found to be 28 nM. Anions such as S^{2-} can also be detected using fluorescent DNA-templated Au/Ag nanoclusters with an LOD for sulfide of 0.83 nM.[58]

Most of the sensing applications involving fluorescent Ag nanoclusters have been carried out in aqueous solutions. Test paper based sensing (analogous to pH paper and blood glucose test strips) may be more convenient for practical field applications. PMAA stabilized Ag nanoclusters synthesized by photochemical reduction have been shown to respond to Cu^{2+} in aqueous solutions.[52] Ag nanoclusters can also be immobilized on cellulose filter paper for label-free detection of Cu^{2+}.[59] After binding to cellulose papers, Ag nanoclusters still maintained their fluorescence toward Cu^{2+} and the decrease of fluorescent signals can be easily observed under UV irradiation (Figure 4.7).[59] Such a paper-based sensing platform provides a new route for using water-soluble fluorescent Ag nanoclusters as optical reporters.

4.3.2 Applications of Ag Nanoclusters in Biosensing

Cysteine (Cys), homocysteine (Hcy), and glutathione (GSH) are important small thiol-containing biomolecules. The thiol groups not only can stabilize

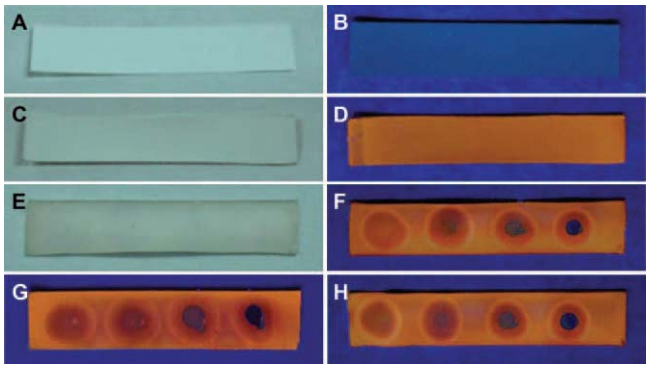

Figure 4.7 Ag nanoclusters on a paper platform for detection of Cu^{2+}: comparisons of the paper strips before (A and B) and after (C and D) immobilization of Ag nanoclusters. The photographs of the test papers after adding different concentrations of Cu^{2+} in (E and F) deionized water, (G) river water, and (H) barreled drinking water, from left to right: 0, 2×10^{-5}, 10^{-4}, 10^{-3} M. (A, C and E) and (B, D and F) are the same strips under white light and UV light illumination, respectively.
Reproduced with permission from ref. 59. Copyright 2012 Royal Society of Chemistry.

Ag nanoclusters but can also induce the oxidation of Ag nanoclusters, which leads to a decrease of fluorescence intensity.[60] A simple fluorescence quenching method was developed for detection of cysteine based on PMAA stabilized Ag nanoclusters.[61] The binding of Cys with Ag nanoclusters can readily induce the quenching of Ag nanoclusters while other á-amino acids do not. This method allowed Ag nanoclusters to selectively detect Cys with a LOD of 20 nM.[61] Due to steric hindrance, large thiol-containing compounds like bovine serum albumin (BSA) and GSH cannot efficiently quench the fluorescence of Ag nanoclusters.

Although the fluorescence of Ag nanoclusters can be efficiently quenched by thiol-containing compounds, in some cases thiols can be used to enhance the fluorescence of Ag nanoclusters. A ''turn-on'' assay was introduced to selectively detect thiol-containing compounds.[62] For example, the fluorescence intensity of Ag nanoclusters prepared with single strand DNA consisting of 12 cytosines can be enhanced in the presence of thiol-containing compounds. This ''turn-on'' approach was able to detect GSH with a LOD at 6.2 nM.[62]

The sequence of DNA can greatly influence the fluorescence of Ag nanoclusters, which permits their broad use for detection of specific DNA sequences, even to a single mutated nucleotide in a double stranded DNA. For example, if a nucleotide mismatch occurred two bases away from the nanocluster formation site (C_6 loop in the duplex), the fluorescence of Ag nanoclusters is quenched.[63] The location of the C_6 loop can be used to tune the fluorescence of Ag nanoclusters: locating the C_6-loop one or two bases away from the mutation site produced the most intense fluorescence,

whereas moving the C_6-loop further from the mutation site, the fluorescence intensity became much weaker.

The fluorescence of DNA-templated Ag nanoclusters can be enhanced in the presence of guanine-rich DNA sequences.[64] This interesting phenomenon can also be exploited for DNA sensing (Figure 4.8).[64] The remaining segment of strand 1 bearing dark (non-fluorescent) Ag nanoclusters was used as a hybridization sequence to pair another single strand. After a guanine-rich complement tail hybridized with strand 1, an intense red emission fluorescence was observed, with emission intensity enhanced up to 500-fold and the enhancement exponentially increased with increasing number of guanine bases in proximity to the Ag nanoclusters. This type of Ag nanocluster can detect target DNA sequences with an exceptionally high signal-to-noise ratio of 175.

Ag nanoclusters have also been developed as fluorescent protein sensors. Aptamer-templated Ag nanoclusters have been synthesized and used for

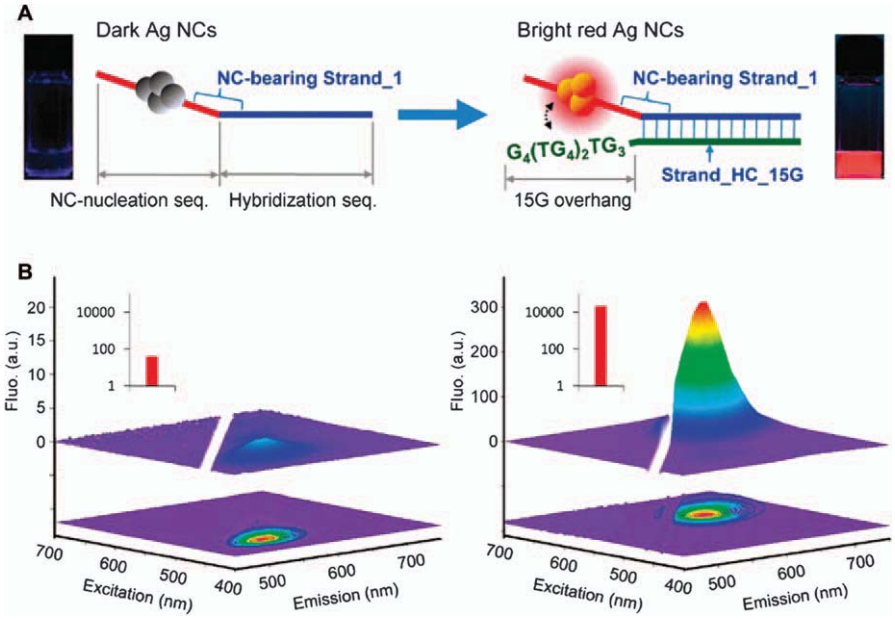

Figure 4.8 (A) Schematic showing the red fluorescence enhancement of DNA–Ag nanoclusters through proximity with a G-rich overhang, 3′-G4(TG4)TG3, caused by DNA hybridization and photographs of the resulting emission under 366 nm UV irradiation. (B) 3D- and 2D-contour plots of excitation/emission spectra of the Ag nanoclusters before (left) and after (right) hybridizing nanocluster-bearing Strand 1 with Strand HC–15G. Inset: Integrated red fluorescence emission subtracted with buffer fluorescence in arbitrary units, which indicates an enhancement of ~500-fold after duplex formation.
Reproduced with permission from ref. 64. Copyright 2010 American Chemical Society.

selective detection of thrombin.[65] A specific DAN scaffold containing a cytosine-rich DNA sequence (12-mer) was used to stabilize fluorescent Ag nanoclusters, and a thrombin-binding aptamer sequence (29-mer) was added to that to recognize thrombin. The fluorescence of the resulting Ag nanoclusters can be quenched *via* target binding of thrombin to the DNA scaffold. The detection limit of thrombin in this method was measured to be 1 nM. DNA-templated highly fluorescent (quantum yield >50%) Ag nanoclusters can be used to detect single-strand DNA binding proteins (SSBs).[66] When SSBs interacted with DNA-templated Ag nanoclusters, the DNA scaffold altered their configurations leading to the quenching of fluorescence, with a resulting LOD of 0.2 nM. This method allowed selective detection of SSBs over other tested proteins, including trypsin, lysozyme, myoglobin, BSA, thrombin, *etc.*

4.4 Conclusions

Water-soluble fluorescent Ag nanoclusters have now emerged as an important class of luminescent nanomaterials. Recent advances in the synthesis of fluorescent Ag nanoclusters *via* various synthetic methodologies have provided insights into the origins of their excellent photophysical properties as well as the development of applications in chemical- and biosensing, bio-imaging, and single molecule microscopy. Ag nanoclusters are among the strongest fluorescent emitters, exhibiting high quantum yields, high emission rates, large Stokes shifts, high molecular extinction coefficients, and excellent photostability. Their fluorescent properties are controlled through the details of their synthesis and stabilizing surface bound polyelectrolytes and are sensitive to the surrounding conditions.

It would be highly desirable to correlate the size of Ag nanoclusters with their corresponding optical properties. Current synthetic approaches cannot precisely allow production of Ag nanoclusters with specific numbers of Ag atoms. Therefore, it is still challenging to develop efficient synthetic routes to prepare truly monodispersed, highly emissive Ag nanoclusters. Although DNA, polyelectrolytes, proteins, and thiol-containing compounds have been used to protect and stabilize Ag nanoclusters, a general understanding of how such surface modifications affect the chemical and physical properties of Ag nanoclusters is still incomplete. Much work remains to be done before we will be able to achieve control over size and surface chemistry of each individual Ag nanocluster.

Another area where Ag nanoclusters may find useful future applications is catalysis. Ag nanoparticles have already been used to catalyze a variety of oxidation reactions[67–69] and Ag nanoclusters deposited on alumina have been demonstrated to catalyze the reduction of various nitro aromatic compounds with good recyclability.[70] Further applications of water-soluble Ag nanoclusters as catalysts in aqueous solutions are likely to continue and expand, and it will be interesting to see if the fluorescent properties of Ag nanoclusters prove useful as mechanistic probes during such catalysis.

References

1. J. Zheng, P. R. Nicovich and R. M. Dickson, *Annu. Rev. Phys. Chem.*, 2007, **58**, 409.
2. J. P. Wilcoxon and B. L. Abrams, *Chem. Soc. Rev.*, 2006, **35**, 1162.
3. I. Diez and R. H. A. Ras, *Nanoscale*, 2011, **3**, 1963.
4. Y. Z. Lu and W. Chen, *Chem. Soc. Rev.*, 2012, **41**, 3594.
5. L. Shang, S. J. Dong and G. U. Nienhaus, *Nano Today*, 2011, **6**, 401.
6. S. Choi, R. M. Dickson and J. H. Yu, *Chem. Soc. Rev.*, 2012, **41**, 1867.
7. Y. C. Shiang, C. C. Huang, W. Y. Chen, P. C. Chen and H. T. Chang, *J. Mater. Chem.*, 2012, **22**, 12972.
8. A. Latorre and A. Somoza, *ChemBioChem*, 2012, **13**, 951.
9. H. X. Xu and K. S. Suslick, *Adv. Mater.*, 2010, **22**, 1078.
10. D. N. Rogers, *Chemistry of Photography*, The Royal Society of Chemistry, Cambridge, 2006.
11. http://www.cheresources.com/content/articles/other-topics/chemistry-of-photography.
12. S. Fedrigo, W. Harbich and J. Buttet, *J. Chem. Phys.*, 1993, **99**, 5712.
13. W. Schulze, I. Rabin and G. Ertl, *ChemPhysChem*, 2004, **5**, 403.
14. A. Henglein, *Chem. Phys. Lett.*, 1989, **154**, 473.
15. T. Linnert, P. Mulvaney, A. Henglein and H. Weller, *J. Am. Chem. Soc.*, 1990, **112**, 4657.
16. A. Henglein, *J. Phys. Chem.*, 1993, **97**, 5457.
17. B. G. Ershov and A. Henglein, *J. Phys. Chem. B*, 1998, **102**, 10663.
18. P. Mulvaney and A. Henglein, *Chem. Phys. Lett.*, 1990, **168**, 391.
19. A. Henglein, P. Mulvaney and T. Linnert, *Faraday Discuss.*, 1991, **92**, 31.
20. M. Treguer, F. Rocco, G. Lelong, A. Le Nestour, T. Cardinal, A. Maali and B. Lounis, *Solid State Sci.*, 2005, **7**, 812.
21. L. A. Peyser, A. E. Vinson, A. P. Bartko and R. M. Dickson, *Science*, 2001, **291**, 103.
22. J. Zheng and R. M. Dickson, *J. Am. Chem. Soc.*, 2002, **124**, 13982.
23. L. Shang and S. J. Dong, *Chem. Commun.*, 2008, 1088.
24. I. Diez, M. Pusa, S. Kulmala, H. Jiang, A. Walther, A. S. Goldmann, A. H. E. Muller, O. Ikkala and R. H. A. Ras, *Angew. Chem., Int. Ed.*, 2009, **48**, 2122.
25. H. Zhang, X. Huang, L. Li, G. W. Zhang, I. Hussain, Z. Li and B. Tian, *Chem. Commun.*, 2012, **48**, 567.
26. J. G. Zhang, S. Q. Xu and E. Kumacheva, *Adv. Mater.*, 2005, **17**, 2336.
27. Z. Shen, H. W. Duan and H. Frey, *Adv. Mater.*, 2007, **19**, 349.
28. P. Riesz and T. Kondo, *Free Radical Biol. Med.*, 1992, **13**, 247.
29. K. S. Suslick, Y. Didenko, M. M. Fang, T. Hyeon, K. J. Kolbeck, W. B. McNamara, M. M. Mdleleni and M. Wong, *Philos. Trans. R. Soc., A*, 1999, **357**, 335.
30. E. Ciawi, J. Rae, M. Ashokkumar and F. Grieser, *J. Phys. Chem. B*, 2006, **110**, 13656.
31. J. H. Bang and K. S. Suslick, *Adv. Mater.*, 2010, **22**, 1039.

32. H. X. Xu, B. W. Zeiger and K. S. Suslick, *Chem. Soc. Rev.*, 2013, **42**, 2555.
33. K. S. Suslick and D. J. Flannigan, *Annu. Rev. Phys. Chem.*, 2008, **59**, 659.
34. H. X. Xu and K. S. Suslick, *ACS Nano*, 2010, **4**, 3209.
35. A. Hoz, A. Díaz-Ortiz and A. Moreno, *Chem. Soc. Rev.*, 2005, **34**, 164.
36. R. Gedye, F. Smith, K. Westaway, H. Ali, L. Baldisera, L. Laberge and J. Rousell, *Tetrahedron Lett.*, 1986, **27**, 279.
37. S. H. Liu, F. Lu and J. J. Zhu, *Chem. Commun.*, 2011, **47**, 2661.
38. R. Q. Li, C. L. Wang, F. Bo, Z. Y. Wang, H. B. Shao, S. H. Xu and Y. P. Cui, *ChemPhysChem*, 2012, **13**, 2097.
39. J. T. Petty, J. Zheng, N. V. Hud and R. M. Dickson, *J. Am. Chem. Soc.*, 2004, **126**, 5207.
40. T. Vosch, Y. Antoku, J. C. Hsiang, C. I. Richards, J. I. Gonzalez and R. M. Dickson, *Proc. Natl. Acad. Sci. U. S. A.*, 2007, **104**, 12616.
41. C. M. Ritchie, K. R. Johnsen, J. R. Kiser, Y. Antoku, R. M. Dickson and J. T. Petty, *J. Phys. Chem. C*, 2007, **111**, 175.
42. B. Sengupta, C. M. Ritchie, J. G. Buckman, K. R. Johnsen, P. M. Goodwin and J. T. Petty, *J. Phys. Chem. C*, 2008, **112**, 18776.
43. E. G. Gwinn, P. O'Neill, A. J. Guerrero, D. Bouwmeester and D. K. Fygenson, *Adv. Mater.*, 2008, **20**, 279.
44. T. Li, L. Zhang, J. Ai, S. Dong and E. Wang, *ACS Nano*, 2011, **5**, 6334.
45. Z. Z. Huang, Y. Tao, F. Pu, J. S. Ren and X. G. Qu, *Chem. – Eur. J*, 2012, **18**, 6663.
46. B. Adhikari and A. Banerjee, *Chem. Mater.*, 2010, **22**, 4364.
47. P. T. K. Chin, M. van der Linden, E. J. Harten, A. Barendregt, M. T. M. Rood, A. J. Koster, F. W. B. Leeuwen, C. M. Donega, A. J. R. Heck and A. Meijerink, *Nanotechnology*, 2013, **24**, 075703.
48. M. A. H. Muhanmmed, F. Aldeek, G. Palui, L. Trapiella-Alfonso and H. Mattoussi, *ACS Nano*, 2012, **6**, 8950.
49. N. Cathcart, P. Mistry, C. Makra, B. Pietrobon, N. Coombs, M. Kelokhani-Niaraki and V. Kitaev, *Langmuir*, 2009, **25**, 5840.
50. S. S. Narayanan and S. K. Pal, *J. Phys. Chem. C*, 2008, **112**, 4874.
51. A. Ledo-Suarez, J. Rivas, C. F. Rodriguez-Abreu, M. J. Rodriguez, E. Pastor, A. Hernandez-Creus, S. B. Oseroff and M. A. Lopez-Quintela, *Angew. Chem., Int. Ed.*, 2007, **46**, 8823.
52. L. Shang and S. J. Dong, *J. Mater. Chem.*, 2008, **18**, 4636.
53. M. Zhang and B. C. Ye, *Analyst*, 2011, **136**, 5139.
54. Y. T. Su, G. Y. Lan, W. Y. Chen and H. T. Chang, *Anal. Chem.*, 2010, **82**, 8566.
55. W. Guo, J. Yuan and E. Wang, *Chem. Commun.*, 2009, 3395.
56. G. Y. Lan, W. Y. Chen and H. T. Chan, *RSC Adv*, 2011, **1**, 802.
57. L. Deng, Z. Zhou, J. Li, T. Li and S. Dong, *Chem. Commun.*, 2011, **47**, 11065.
58. W. Y. Chen, G. Y. Lan and H. T. Chan, *Anal. Chem.*, 2011, **83**, 9450.
59. X. J. Liu, C. H. Zong and L. H. Lu, *Analyst*, 2012, **137**, 2406.
60. B. Y. Han and E. Wang, *Biosens. Bioelectron.*, 2011, **26**, 2585.
61. L. Shang and S. J. Dong, *Biosens. Bioelectron.*, 2009, **24**, 1569.

62. Z. Z. Huang, F. Pu, Y. Lin, J. S. Ren and X. Qu, *Chem. Commun.*, 2011, **47**, 3487.
63. W. Guo, J. Yuan, Q. Dong and E. Wang, *J. Am. Chem. Soc.*, 2010, **132**, 932.
64. H. C. Yeh, J. Sharma, J. J. Han, J. S. Martinez and J. H. Werner, *Nano Lett.*, 2010, **10**, 3106.
65. J. Sharma, H. C. Yeh, H. Yoo, J. H. Werner and J. S. Martinez, *Chem. Commun.*, 2011, **47**, 2294.
66. G. Y. Lan, W. Y. Chen and H. T. Chang, *Analyst*, 2011, **136**, 3623.
67. K. Watanabe, D. Menzel, N. Nilius and H. J. Freund, *Chem. Rev.*, 2006, **106**, 4301.
68. Y. Y. Chen, C. Wang, H. Y. Liu, J. S. Qiu and X. H. Bao, *Chem. Commun.*, 2005, 5298.
69. T. Mitsudome, S. Arita, H. Mori, T. Mizugaki, K. Jitsukawa and K. Kaneda, *Angew. Chem., Int. Ed.*, 2008, **47**, 138.
70. A. Leelavathi, T. U. B. Rao and T. Pradeep, *Nanoscale Res. Lett.*, 2011, **6**, 1.